

Energy fluxes in helical magnetohydrodynamics and dynamo action

Mahendra K. Verma

Department of Physics, Indian Institute of Technology, Kanpur { 208016, INDIA

(Dated: Nov. 26, 2001)

Renormalized viscosity, renormalized resistivity, and various energy fluxes are calculated for helical magnetohydrodynamics using perturbative field theory. The calculation is to first-order in perturbation. Kinetic and magnetic helicities do not affect the renormalized parameters, but they induce an inverse cascade of magnetic energy. Based on our flux results, a dynamically consistent model for galactic dynamo has been constructed. Here the sources for the large-scale magnetic field growth have been shown to be (1) energy flux from large-scale velocity field to large-scale magnetic field arising due to nonhelical interactions, and (2) inverse energy flux of magnetic energy caused by helical interactions. Our calculations yields dynamo time-scale for a typical galaxy to be of the order of 10^8 years. Our field-theoretic calculations also reveal that the flux of magnetic helicity is backward, consistent with the earlier observations based on absolute equilibrium theory.

PACS numbers: PACS numbers: 47.27.Gs, 52.35.Ra, 91.25.Cw

I. INTRODUCTION

Generation of magnetic field in plasma, usually referred to as "dynamo", is one of the prominent and unsolved problems in physics and astrophysics. It is known that the magnetic field of galaxies, the Sun, and the Earth are neither due to some permanent magnet nor due to any remnants of the past, but it is generated by the nonlinear processes of plasma motion ([1, 2] and references therein). However, a solid quantitative understanding is lacking in this area. In this paper and in paper I ([3]) we address the above problem by computing the energy exchanges between velocity and magnetic field using field-theoretic methods in a somewhat idealized environment, homogeneous and isotropic flows. In paper I we show that the nonhelical part of magnetohydrodynamic (MHD) interaction causes energy transfer from large-scale (LS) velocity field to large-scale (LS) magnetic field. In a typical dynamo environment however, the helical interactions cause an additional energy cascade of magnetic energy from small scales (SS) to large scales; the field-theoretic calculation of helical contribution to the energy flux is presented in this paper. Both helical and nonhelical factors contribute to the magnetic energy growth.

In the problem of magnetic field generation, it is required that the LS magnetic field is maintained at all time. There are several exact results in this area, e.g., dynamo does not exist in two dimensions as well as in axisymmetric flows [1]. In the past, several dynamos, e.g., rotor dynamo, 2-sphere dynamo etc., have been constructed [1], however, mean-field electrodynamics developed by Steenbeck et al. [4] (also see Krause and Radler [2]) paved a way for practical calculations in astrophysical and terrestrial dynamo. This formalism also provided insights into the physical mechanism of dynamo, mainly that kinetic helicity H_K ($\int \mathbf{u} \cdot \boldsymbol{\omega}$, where \mathbf{u} and $\boldsymbol{\omega}$ are the velocity and vorticity fields respectively) plays an important role in the amplification of the magnetic field. The amplification parameter σ was found to be $\sigma = 3H_K$, where τ is the velocity de-correlation time.

Mean-field electrodynamics of Steenbeck et al. [4] is a kinematic theory. Here it is assumed that the velocity field is a known function, which is unaffected by the generated magnetic field. The later models which take into account the back reaction of the magnetic field to the velocity field are called dynamic models. One of the first dynamic model is due to Pouquet et al. [5] where they incorporated the feedback, and proposed that the modified σ is proportional to residual helicity, $H_K - H_J$, where H_J is the current helicity defined by Liberman and Gruzinov and Diamond [6] proposed a quenching mechanism where the amplification parameter was modified to

$$\sigma = \frac{\sigma_0}{1 + R_m \overline{(\mathbf{B} \cdot \nabla \times \mathbf{u})^2}} \quad (1)$$

where $\overline{B^2}$ is the LS magnetic energy, \overline{U} is the LS velocity field, and R_m is the magnetic Reynolds number. Recently Field, Blackman, and Chou [7], and Chou [8] obtained a general expression for dynamic coefficient as a function of Reynolds number and magnetic Prandtl number.

There are many numerical simulations of dynamo in various geometries. In simulations MHD equations are numerically solved with appropriate boundary conditions. In this paper we will only refer to the simulations performed for a periodic box; this is to avoid the complications of spherical geometry (e.g., effects of Coriolis force etc.). Pouquet et al. [5] numerically integrated the MHD equations on the basis of Eddy-damped-quasi-normal-Markovian (EDQNM) approximation. When kinetic energy (KE) and H_K were injected near a wavenumber band, both magnetic energy (ME) and absolute value of magnetic helicity $|H_M|$ were found to increase. Note however that one part of the time-scale used in Pouquet et al.'s calculation is based on Alfvén relaxation time. This assumption is suspect in view of

current theoretical [9, 10, 11, 12, 13] and numerical results [14, 15, 16], which favour $k^{-5/3}$ (Kolmogorov's) energy spectrum over Kraichnan's $k^{-3/2}$ spectrum for MHD turbulence. In our present paper, the nonlinear time-scale is based on Kolmogorov's energy spectrum. The direct numerical simulation (DNS) of Pouquet and Patterson [17] yielded a similar result. Recently, Brandenburg [18] has numerically solved the compressible MHD equations with helicity. He also observed a growth of the LS magnetic energy before it saturates. Frick and Sokolov [19] studied the shell model of turbulence, and showed that magnetic helicity suppresses turbulent cascade.

In another development Dar et al. [20] numerically calculated various energy fluxes in two-dimensional MHD and showed that there is significant energy transfer from LS velocity field to LS magnetic field; they claimed that the above flux is one of the main contributors to the amplification of large-scale ME. Note that the ratio ME/KE grows in both helical and nonhelical MHD as well as in many decaying as well as forced simulations (see for example, [20, 21] and references therein). Hence, helicity is not a necessary requirement for the generation of magnetic energy. Regarding flux of magnetic helicity, Pouquet et al. [5] and Pouquet and Patterson [17] argue that it is in the inverse direction (from SS to LS). We find a similar magnetic helicity flux in our theoretical calculation.

In one of the recent theoretical developments Kulsrud and Anderson [22] derived and solved the kinetic equation for the growth of galactic magnetic field. They argued that the dynamo time-scale is much larger than the growth time-scale of turbulent modes. Hence, the buildup of SS turbulent ME dominates the slow growth of LS ME, thus making the mean dynamo theory invalid.

In paper I and the present paper, the energy fluxes of MHD turbulence are computed using perturbative field theory. The calculation is to first order in perturbation. Here the viscosity and resistivity were taken from renormalization calculation of Verma [12, 13], and the energy spectrum were taken to Kolmogorov-like ($k^{-5/3}$). Kolmogorov's spectrum for MHD turbulence is supported by recent theoretical [9, 10, 11, 12, 13] and numerical results [14, 15, 16]. In paper I we show that in a kinetically forced nonhelical MHD, the energy transfer from LS velocity field to LS magnetic field is one of the dominant transfers. It is also shown in paper I that the above energy flux into LS magnetic modes is independent of the nature of LS forcing. In this paper we generalize the field-theoretic calculation of Verma [3, 12] to helical MHD. As discussed in paper I, we assume that the turbulence is homogeneous and isotropic, and that the mean magnetic field is absent. The absence of mean magnetic field is a reasonable assumption for the initial stages of dynamo evolution. This assumption is to ensure that the turbulence is isotropic. In addition we take cross helicity ($2\mathbf{u} \cdot \mathbf{b}$) to be zero to simplify the calculation. We examine the fluxes in the presence of magnetic and kinetic helicities. We also investigate the flux of magnetic helicity.

We have constructed a dynamo model using the theoretically-calculated energy flux into the large-scale magnetic field. In this model the ME grows exponentially in the initial stage, and the growth time-scale is of the order of eddy turnover time. It shows that dynamo action is possible in galactic dynamo.

The outline of the paper is as follows: in section 2, we carry out the perturbative calculation of renormalized viscosity and resistivity, as well as fluxes of energy and magnetic helicity. In section 3, we construct a dynamic galactic dynamo based on our energy flux results. In this section we also compare our results with the findings of earlier researchers. Section 4 contains conclusions.

II. FIELD-THEORETIC CALCULATION OF HELICAL MAGNETOHYDRODYNAMICS

The incompressible MHD equation in Fourier space is given by

$$i! + k^2 u_i(\hat{k}) = \frac{i}{2} P_{ijm}^+(\mathbf{k}) \int \frac{d\hat{p}}{Z} [u_j(\hat{p})u_m(\hat{k}-\hat{p}) - b_j(\hat{p})b_m(\hat{k}-\hat{p})] \quad (2)$$

$$i! + k^2 b_i(\hat{k}) = iP_{ijm}(\mathbf{k}) \int \frac{d\hat{p}}{Z} [u_j(\hat{p})b_m(\hat{k}-\hat{p})] \quad (3)$$

$$k_i u_i(\mathbf{k}) = 0 \quad (4)$$

$$k_i b_i(\mathbf{k}) = 0 \quad (5)$$

where u and b are the velocity and magnetic field fluctuations respectively, and ν and η are the viscosity and the resistivity respectively, and

$$P_{ijm}^+(\mathbf{k}) = k_j P_{im}(\mathbf{k}) + k_m P_{ij}(\mathbf{k}); \quad (6)$$

$$P_{im}(\mathbf{k}) = \nu_{im} \frac{k_i k_m}{k^2}; \quad (7)$$

$$P_{ijm}(\mathbf{k}) = k_j \nu_{im} - k_m \nu_{ij}; \quad (8)$$

$$\hat{k} = (\mathbf{k}; !); \quad d\hat{p} = d\mathbf{p} d! = (2\pi)^4; \quad (9)$$

Note that we are working in three space dimension and also with zero mean magnetic field.

Some of the definitions regarding kinetic and magnetic helicities are in order. Throughout this paper, \mathbf{a} denotes the vector potential ($\mathbf{b} = \nabla \times \mathbf{a}$), and $\boldsymbol{\omega}$ denotes the vorticity ($\boldsymbol{\omega} = \nabla \times \mathbf{u}$). The spectrum of helicity, $H_M(\mathbf{k})$, is defined using the equal-time correlation function $\langle \mathbf{h}_i(\mathbf{k}; t) \mathbf{b}_j(\mathbf{k}^0; t) \rangle$ (the angular brackets denote ensemble average),

$$\langle \mathbf{h}_i(\mathbf{k}; t) \mathbf{b}_j(\mathbf{k}^0; t) \rangle \stackrel{\text{def}}{=} P_{ij}(\mathbf{k}) H_M(\mathbf{k}; t) (\mathbf{k} + \mathbf{k}^0) \quad (10)$$

The factor $P_{ij}(\mathbf{k})$ appears due to the constraints $\nabla \cdot \mathbf{a} = \nabla \cdot \mathbf{b} = 0$. Using this correlation function we derive the following relationship:

$$\begin{aligned} H_M &= \frac{1}{2} \int \langle \mathbf{h}_i(\mathbf{x}) \cdot \mathbf{b}(\mathbf{x}) \rangle d\mathbf{x} \\ &= \frac{1}{2} \int \frac{d\mathbf{k}}{(2\pi)^3} \frac{d\mathbf{k}^0}{(2\pi)^3} \langle \mathbf{h}_i(\mathbf{k}) \cdot \mathbf{b}(\mathbf{k}^0) \rangle \\ &= \frac{d\mathbf{k}}{(2\pi)^3} H_M(\mathbf{k}) \end{aligned} \quad (11)$$

The one-dimensional magnetic helicity $H_M(k)$ is defined using

$$H_M(k) dk = \int \frac{d\mathbf{k}}{(2\pi)^3} H_M(\mathbf{k}) \quad (12)$$

Therefore,

$$H_M(k) = \frac{4\pi k^2}{(2\pi)^3} H_M(k) \quad (13)$$

Using $\nabla \times \mathbf{a} = \mathbf{b}$ we can easily derive that

$$\mathbf{a}(\mathbf{k}) = \frac{i}{k^2} \mathbf{k} \times \mathbf{b}(\mathbf{k}) \quad (14)$$

which leads to

$$\langle \mathbf{h}_i(\mathbf{k}) \mathbf{b}_j(\mathbf{k}^0) \rangle = P_{ij}(\mathbf{k}) C^{bb}(\mathbf{k}) - \frac{1}{2} \delta_{ij} k_1^2 H_M(\mathbf{k}) (\mathbf{k} + \mathbf{k}^0) \quad (15)$$

where C^{bb} is the $\mathbf{b} \cdot \mathbf{b}$ correlation function.

A similar analysis for kinetic helicity shows that

$$\langle \mathbf{h}_i(\mathbf{k}) \boldsymbol{\omega}_j(\mathbf{k}^0) \rangle \stackrel{\text{def}}{=} P_{ij}(\mathbf{k}) H_K(\mathbf{k}) (\mathbf{k} + \mathbf{k}^0) \quad (16)$$

$$H_K = \frac{1}{2} \int \langle \mathbf{h}_i \cdot \boldsymbol{\omega}_i \rangle d\mathbf{x} = \frac{d\mathbf{k}}{(2\pi)^3} H_K(\mathbf{k}) \quad (17)$$

and

$$\langle \mathbf{h}_i(\mathbf{k}) \mathbf{u}_j(\mathbf{k}^0) \rangle = P_{ij}(\mathbf{k}) C^{uu}(\mathbf{k}) - \frac{1}{2} \delta_{ij} k_1 \frac{2H_K(\mathbf{k})}{k^2} (\mathbf{k} + \mathbf{k}^0) \quad (18)$$

where C^{uu} is the $\mathbf{u} \cdot \mathbf{u}$ correlation function.

An important point to note is that magnetic helicity is conserved in MHD when $\eta = \nu = 0$. One of the consequences of this conservation law is the emergence of k^{-1} spectrum at small wavenumbers [23]. The kinetic helicity is conserved in fluid turbulence, but not in MHD turbulence.

In the following subsection we will calculate the renormalized viscosity and resistivity for helical MHD.

A . Calculation of renormalized parameters

Recently Verma [12, 13] has calculated the renormalized viscosity and resistivity for MHD turbulence in absence of kinetic and magnetic helicity. It will be shown below that the presence of both kinetic and magnetic helicities does not alter the renormalized viscosity and resistivity calculated for nonhelical MHD.

In the RG procedure the wavenumber range $(k_N; k_0)$ is divided logarithmically into N shells. Then the elimination of the first shell $k^> = (k_1; k_0)$ is carried out and the modified MHD equation for $k^< = (k_N; k_1)$ is obtained. This process is continued for higher shells. The shell elimination is performed by ensemble averaging over $k^>$ modes [12, 13, 24]. It is assumed that $u_i^>(\hat{k})$ and $b_i^>(\hat{k})$ have gaussian distributions with zero mean, while $u_i^<(\hat{k})$ and $b_i^<(\hat{k})$ are unaffected by the averaging process. In addition it is also assumed that

$$u_i^>(\phi)u_j^>(\phi) = P_{ij}(\phi)C^{uu}(\phi) - i_{ij1}\frac{P_1}{P^2}2H_K(\phi) \quad (\phi + \phi) \quad (19)$$

$$b_i^>(\phi)b_j^>(\phi) = P_{ij}(\phi)C^{bb}(\phi) - i_{ij1}P_12H_M(\phi) \quad (\phi + \phi) \quad (20)$$

Note that u - b correlation has been taken to be zero in our calculation.

We apply first-order perturbation theory to compute the renormalized parameters. After elimination of n shells, we obtain the following equations for the renormalized viscosity $\nu^{(n)}$ and renormalized resistivity $\eta^{(n)}$ (for details refer to Verma [13]).

$$i! + \nu^{(n)}k^2 + \nu^{(n)}k^2 u_i^<(\hat{k}) = \frac{i}{2}P_{ijm}^+(\mathbf{k}) \int_{\mathcal{Z}} d\phi [u_j^<(\phi)u_m^<(\hat{k} - \phi) b_j^<(\phi)b_m^<(\hat{k} - \phi)] \quad (21)$$

$$i! + \nu^{(n)}k^2 + \nu^{(n)}k^2 b_i^<(\hat{k}) = iP_{ijm}(\mathbf{k}) \int_{\mathcal{Z}} d\phi [u_j^<(\phi)b_m^<(\hat{k} - \phi)] \quad (22)$$

where

$$\nu^{(n)}(\mathbf{k}) = \frac{1}{2k^2} \int_{\mathcal{Z}} \frac{d\mathbf{p}}{p+q=\hat{k}} \frac{1}{(2)^3} \frac{S(\mathbf{k};\mathbf{p};\mathbf{q})C^{uu}(\mathbf{q}) + S^0(\mathbf{k};\mathbf{p};\mathbf{q})H_K(\mathbf{q})}{\nu^{(n)}(\mathbf{p})p^2 + \nu^{(n)}(\mathbf{q})q^2} + \frac{S_6(\mathbf{k};\mathbf{p};\mathbf{q})C^{bb}(\mathbf{q}) + S_6^0(\mathbf{k};\mathbf{p};\mathbf{q})H_M(\mathbf{q})}{\nu^{(n)}(\mathbf{p})p^2 + \nu^{(n)}(\mathbf{q})q^2} \quad (23)$$

$$\eta^{(n)}(\mathbf{k}) = \frac{1}{2k^2} \int_{\mathcal{Z}} \frac{d\mathbf{p}}{p+q=\hat{k}} \frac{1}{(2)^3} \frac{S_8(\mathbf{k};\mathbf{p};\mathbf{q})C^{bb}(\mathbf{q}) + S_8^0(\mathbf{k};\mathbf{p};\mathbf{q})H_M(\mathbf{q})}{\nu^{(n)}(\mathbf{p})p^2 + \nu^{(n)}(\mathbf{q})q^2} + \frac{S_9(\mathbf{k};\mathbf{p};\mathbf{q})C^{uu}(\mathbf{q}) + S_9^0(\mathbf{k};\mathbf{p};\mathbf{q})H_K(\mathbf{q})}{\nu^{(n)}(\mathbf{p})p^2 + \nu^{(n)}(\mathbf{q})q^2} \quad (24)$$

The quantities S_i and S_i^0 are as follows:

$$S(\mathbf{k};\mathbf{p};\mathbf{q}) = P_{bjm}^+(\mathbf{k})P_{mab}^+(\mathbf{p})P_{ja}(\mathbf{q}) = 2kpz^3 + xy \quad (25)$$

$$S_6(\mathbf{k};\mathbf{p};\mathbf{q}) = P_{ajm}^+(\mathbf{k})P_{mba}^+(\mathbf{p})P_{jb}(\mathbf{q}) = 2kpz - 1 - y^2 \quad (26)$$

$$S_8(\mathbf{k};\mathbf{p};\mathbf{q}) = P_{ijm}(\mathbf{k})P_{jab}^+(\mathbf{p})P_{ma}(\mathbf{q})P_{ib}(\mathbf{k}) = S_6(\mathbf{p};\mathbf{k};\mathbf{q}) \quad (27)$$

$$S_9(\mathbf{k};\mathbf{p};\mathbf{q}) = P_{ijm}(\mathbf{k})P_{mab}^+(\mathbf{p})P_{ja}(\mathbf{q})P_{ib}(\mathbf{k}) = 2kp(z + xy) \quad (28)$$

$$S^0(\mathbf{k};\mathbf{p};\mathbf{q}) = P_{bjm}^+(\mathbf{k})P_{mab}^+(\mathbf{p})P_{ja1}q_1 = 0 \quad (29)$$

$$S_6^0(\mathbf{k};\mathbf{p};\mathbf{q}) = P_{ajm}^+(\mathbf{k})P_{mba}^+(\mathbf{p})P_{ja1}q_1 = 0 \quad (30)$$

$$S_8^0(\mathbf{k};\mathbf{p};\mathbf{q}) = P_{ijm}(\mathbf{k})P_{jab}^+(\mathbf{p})P_{ma1}q_1P_{ib}(\mathbf{k}) = 0 \quad (31)$$

$$S_9^0(\mathbf{k};\mathbf{p};\mathbf{q}) = P_{ijm}(\mathbf{k})P_{mab}^+(\mathbf{p})P_{ja1}q_1P_{ib}(\mathbf{k}) = 0 \quad (32)$$

Since all $S_i^0(\mathbf{k};\mathbf{p};\mathbf{q})$ turn out to be zero, the presence of helicities does not alter the already calculated $\nu^{(n)}$ and $\eta^{(n)}$ ($\nu^{(n)}$ and $\eta^{(n)}$) (\mathbf{k}) by Verma [12, 13]¹. Zhou [25] arrived at a similar conclusion while calculating the renormalized viscosity for helical uid

¹ Since ν and η are proper scalars and $H_{M,K}$ are pseudo scalars, $S_i^0(\mathbf{k};\mathbf{p};\mathbf{q})$ will be pseudo scalars. In addition, $S_i^0(\mathbf{k};\mathbf{p};\mathbf{q})$ are also linear in \mathbf{k} , \mathbf{p} and \mathbf{q} . This implies that $S_i^0(\mathbf{k};\mathbf{p};\mathbf{q})$ must be proportional to $q_1(\mathbf{k} - \mathbf{p})$, which will be zero because $\mathbf{k} = \mathbf{p} + \mathbf{q}$.

turbulence.

Verná [12, 13] obtained a self-consistent solution of the renormalized parameters using Kolmogorov's spectrum. Since the helicities do not alter the renormalized parameters, we arrive at the same formula for renormalized viscosity and resistivity as Verná [12, 13], that is,

$$(\nu; \eta)(k) = \begin{cases} (K^u)^{1=2} \quad 1=3 k \quad 4=3 (\nu; \eta) & \text{for } k < k_n \\ (K^u)^{1=2} \quad 1=3 k_n \quad 4=3 (\nu; \eta) & \text{for } k > k_n \end{cases} \quad (33)$$

where ν and η are the renormalized parameters. The value of these renormalized parameters have been listed in [12, 13].

The present calculation has been carried out up to first order. The probability distribution of velocity is gaussian, while that of velocity difference is nongaussian. The nongaussian behaviour of velocity difference has significant effects specially on higher order structure functions, which are not properly accounted for by first order calculations. Yet, the first order calculation of renormalized viscosity yields results very close to those obtained in experiments and numerical simulations (see e.g., [24, 26]). For the above reason, we have stuck to the first-order field-theoretic calculation in the present paper.

In the next subsection we will calculate the energy and helicity fluxes using the field theoretic technique.

B. Calculation of energy and helicity fluxes

In paper I we have analytically calculated energy fluxes in the absence of magnetic and kinetic helicities. In this subsection we will generalize that calculation for helical MHD. Refer to paper I for the energy evolution equations and other basic formulas.

As discussed in paper I, the energy flux from inside of the X-sphere ($k < k_0$) to outside of the Y-sphere ($k > k_0$) is

$$\mathcal{S}_{Y>}^{X<}(k_0) = \int_{k^0 > k_0}^Z \frac{dk^0}{(2\pi)^3} \int_{p < k_0}^Z \frac{dp}{(2\pi)^3} S^{YX}(k^0, \mathbf{p}, \mathbf{q}) \quad (34)$$

where X and Y stand for u or b, and $S(k^0, \mathbf{p}, \mathbf{q})$ is energy transfer from mode p of X field to mode k of Y field, with mode q acting as a mediator. We calculate the above fluxes analytically to the leading order in perturbation series using the same procedure as in paper I. Some additional terms appear in $\mathcal{H}S(k^0, \mathbf{p}, \mathbf{q})$ due to the presence of helicity. The expressions for S^{YX} for helical MHD are

$$\begin{aligned} \mathcal{H}S^{uu}(k^0, \mathbf{p}, \mathbf{q}) &= \int_1^Z dt^0 [T_1(k; p; q) G^{uu}(k; t^0) C^u(p; t^0) C^u(q; t^0) \\ &\quad + T_1^0(k; p; q) G^{uu}(k; t^0) \frac{H_K(p; t^0) H_K(q; t^0)}{p^2 q^2} \\ &\quad + T_5(k; p; q) G^{uu}(p; t^0) C^u(k; t^0) C^u(q; t^0) \\ &\quad + T_5^0(k; p; q) G^{uu}(p; t^0) \frac{H_K(k; t^0) H_K(q; t^0)}{k^2 q^2} \\ &\quad + T_9(k; p; q) G^{uu}(q; t^0) C^u(k; t^0) C^u(p; t^0) \\ &\quad + T_9^0(k; p; q) G^{uu}(q; t^0) \frac{H_K(k; t^0) H_K(p; t^0)}{k^2 p^2} \end{aligned} \quad (35)$$

$$\begin{aligned} S^{ub}(k^0, \mathbf{p}, \mathbf{q}) &= \int_1^Z dt^0 [T_2(k; p; q) G^{uu}(k; t^0) C^b(p; t^0) C^b(q; t^0) \\ &\quad + T_2^0(k; p; q) G^{uu}(k; t^0) H_M(p; t^0) H_M(q; t^0) \\ &\quad + T_7(k; p; q) G^{bb}(p; t^0) C^u(k; t^0) C^b(q; t^0) \\ &\quad + T_7^0(k; p; q) G^{bb}(p; t^0) \frac{H_K(k; t^0)}{k^2} H_M(q; t^0) \\ &\quad + T_{11}(k; p; q) G^{uu}(q; t^0) C^u(k; t^0) C^b(p; t^0) \\ &\quad + T_{11}^0(k; p; q) G^{uu}(q; t^0) \frac{H_K(k; t^0)}{k^2} H_M(p; t^0) \end{aligned} \quad (36)$$

$$S^{bu}(k^0, \mathbf{p}, \mathbf{q}) = \int_1^Z dt^0 [T_3(k; p; q) G^{bb}(k; t^0) C^u(p; t^0) C^b(q; t^0)$$

$$\begin{aligned}
& + T_3^0(k;p;q)G^{bb}(k;t-t^0)\frac{H_K(p;t;t^0)}{p^2}H_M(q;t;t^0) \\
& + T_6(k;p;q)G^{uu}(p;t-t^0)C^b(k;t;t^0)C^b(q;t;t^0) \\
& + T_6^0(k;p;q)G^{uu}(p;t-t^0)H_M(k;t;t^0)H_M(q;t;t^0) \\
& + T_{12}(k;p;q)G^{bb}(q;t-t^0)C^b(k;t;t^0)C^u(p;t;t^0) \\
& + T_{12}^0(k;p;q)G^{bb}(q;t-t^0)H_M(k;t;t^0)\frac{H_K(p;t;t^0)}{p^2} \\
S^{bb}(k^0;\hat{p};\hat{q}) = & \int_1^Z dt^0 T_4(k;p;q)G^{bb}(k;t-t^0)C^b(p;t;t^0)C^u(q;t;t^0) \\
& + T_4^0(k;p;q)G^{bb}(k;t-t^0)H_M(p;t;t^0)\frac{H_K(q;t;t^0)}{q^2} \\
& + T_8(k;p;q)G^{bb}(p;t-t^0)C^b(k;t;t^0)C^u(q;t;t^0) \\
& + T_8^0(k;p;q)G^{bb}(p;t-t^0)H_M(k;t;t^0)\frac{H_K(q;t;t^0)}{q^2} \\
& + T_{10}(k;p;q)G^{uu}(q;t-t^0)C^b(k;t;t^0)C^b(p;t;t^0) \\
& + T_{10}^0(k;p;q)G^{uu}(q;t-t^0)H_M(k;t;t^0)H_M(p;t;t^0)] \quad (37)
\end{aligned}$$

where $T_i(k;p;q)$ are given in paper I. To obtain $T_i^0(k;p;q)$ (helical part) we replace all the second rank tensors of the type $P_{ja}(k)$ by $\epsilon_{jal}k_l$.

The energy flux calculation is upto first order. The assumptions in the above procedure is similar to those of EDQNM calculations. Here the nongaussian behaviour of velocity fluctuations are treated only upto leading order.

A formula for the magnetic helicity flux can be derived in a similar manner. From Eqs. (2,3) we can easily obtain the equation for the evolution of magnetic helicity, which is

$$\frac{\partial H_M(k)}{\partial t} = \frac{1}{2(k+k^0)} \langle b(k) \frac{\partial a(k^0)}{\partial t} + a(k) \frac{\partial b(k^0)}{\partial t} \rangle \quad (39)$$

$$= \frac{1}{2(k+k^0)} S^{H_M}(k^0;\hat{p};\hat{q}) + S^{H_M}(k^0;\hat{q};\hat{p}) \quad (40)$$

where

$$\begin{aligned}
S^{H_M}(k^0;\hat{p};\hat{q}) = & \frac{1}{4} \langle [b(k^0) \cdot (v(p) \cdot b(q))] \\
& + \frac{1}{4} = [k^0 \cdot b(q)a(k) \cdot u(p) \cdot k \cdot u(q)a(k) \cdot b(p)] \quad (41)
\end{aligned}$$

Here $\langle ()$ and $= ()$ stand for real and imaginary part of the arguments, respectively. The quantity $S^{H_M}(k^0;\hat{q};\hat{p})$ can be obtained from the above expression by interchanging p and q . After some algebraic manipulation it can be shown that

$$\begin{aligned}
& S^{H_M}(k^0;\hat{p};\hat{q}) + S^{H_M}(k^0;\hat{q};\hat{p}) + S^{H_M}(p;\hat{k}^0;\hat{q}) \\
& + S^{H_M}(p;\hat{q};\hat{k}^0) + S^{H_M}(q;\hat{k}^0;\hat{p}) + S^{H_M}(q;\hat{p};\hat{k}^0) = 0 \quad (42)
\end{aligned}$$

It shows that the "detailed conservation of magnetic helicity" holds in a triad interaction (when $\epsilon = 0$) [27].

The transfer rate of magnetic helicity from a wavenumber sphere of radius k_0 is

$$H_M(k_0) = \int_{k^0 > k_0}^Z \frac{dk^0}{(2)^3} \int_{p < k_0}^Z \frac{dp}{(2)^3} S^{H_M}(k^0;\hat{p};\hat{q}) \quad (43)$$

The quantity $S^{H_M}(k^0;\hat{p};\hat{q})$ upon simplification yields

$$\begin{aligned}
S^{H_M}(k^0;\hat{p};\hat{q}) = & \frac{1}{2} \langle [_{ijm} \epsilon_{ijm} b_i(k^0) u_j(p) b_m(q) i \\
& + _{jlm} \frac{k_i k_l}{k^2} h u_i(q) b_m(k^0) b_j(p) i \\
& + _{jlm} \frac{k_i k_l}{k^2} h b_i(q) b_m(k^0) u_j(p) i ; \quad (44)
\end{aligned}$$

which is computed perturbatively to the first order. The corresponding Feynman diagrams are

$$S^{H_M}(k^0; \underline{p}, \underline{q}) =$$

The equation shows a sum of nine Feynman diagrams arranged in three rows of three. Each diagram consists of a circle with a horizontal line through its center. The top half of the circle is shaded. The horizontal line is either solid or dashed. The vertices on the horizontal line are either empty triangles (pointing left or right) or shaded triangles. The vertices on the circle are either empty circles or shaded circles. The diagrams are separated by plus signs. The entire sum is labeled (45) on the right.

Here empty, shaded, and filled triangles (vertices) represent i_{jm} ; $i_{jm} k_i k_1 = k^2$ and $i_{jm} k_i k_1 = k^2$ respectively. The empty and filled circles (vertices) denote $(i=2)P_{ijm}$ and iP_{ijm}^+ respectively. When we substitute $h_{i_j} u_{j_i}; h_{i_j} b_{j_i}$ using Eqs. (18,15), we obtain terms involving $C^X(p; t; t^0) H_{(M, K)}(q; t; t^0)$. The resulting expression for $S^{H_M}(k^0; \underline{p}, \underline{q})$ is

$$S^{H_M}(k^0; \underline{p}, \underline{q}) = \int_1^{Z_t} dt^0 T_{31}(k; p; q) G^{bb}(k; t^0) \frac{H_K(p; t^0)}{p^2} C^b(q; t^0)$$

$$+ T_{32}(k; p; q) G^{bb}(k; t^0) C^{uu}(p; t^0) H_M(q; t^0)$$

$$+ T_{33}(k; p; q) G^{uu}(p; t^0) H_M(k; t^0) C^{bb}(q; t^0)$$

$$+ T_{34}(k; p; q) G^{uu}(p; t^0) C^{bb}(k; t^0) H_M(q; t^0)$$

$$+ T_{35}(k; p; q) G^{bb}(q; t^0) H_M(k; t^0) C^{uu}(p; t^0)$$

$$+ T_{36}(k; p; q) G^{bb}(q; t^0) C^{bb}(k; t^0) \frac{H_K(p; t^0)}{p^2}$$

$$+ T_{37}(k; p; q) G^{bb}(k; t^0) H_M(p; t^0) C^{uu}(q; t^0)$$

$$+ T_{38}(k; p; q) G^{bb}(k; t^0) C^{bb}(p; t^0) \frac{H_K(q; t^0)}{q^2}$$

$$+ T_{39}(k; p; q) G^{bb}(p; t^0) H_M(k; t^0) C^{uu}(q; t^0)$$

$$+ T_{40}(k; p; q) G^{bb}(p; t^0) C^{bb}(k; t^0) \frac{H_K(q; t^0)}{q^2}$$

$$+ T_{41}(k; p; q) G^{uu}(q; t^0) H_M(k; t^0) C^{bb}(p; t^0)$$

$$+ T_{42}(k; p; q) G^{uu}(q; t^0) C^{bb}(k; t^0) H_M(p; t^0) g$$

$$+ T_{43}(k; p; q) G^{bb}(k; t^0) \frac{H_K(p; t^0)}{p^2} C^{bb}(q; t^0)$$

$$+ T_{44}(k; p; q) G^{bb}(k; t^0) C^{uu}(p; t^0) H_M(q; t^0) g$$

$$+ T_{45}(k; p; q) G^{uu}(p; t^0) H_M(k; t^0) C^{bb}(q; t^0)$$

$$+ T_{46}(k; p; q) G^{uu}(p; t^0) C^{bb}(k; t^0) H_M(q; t^0)$$

$$+ T_{47}(k; p; q) G^{bb}(q; t^0) H_M(k; t^0) C^{uu}(p; t^0)$$

$$+ T_{48}(k; p; q) G^{bb}(q; t^0) C^{bb}(k; t^0) \frac{H_K(p; t^0)}{p^2}$$
(46)

The terms $T_{31::48}(k;p;q)$ can be obtained in terms of antisymmetric tensors ϵ_{ja1}, P_{ijm} etc. They have not been listed here due to lack of space.

For $G(k;t-t^0)$ of the formulas (35-38,46), we substitute

$$G^{(uu;bb)}(k;t-t^0) = \exp\left(-\frac{(k);(k)}{k^2}(t-t^0)\right) \quad (47)$$

where $(k);(k)$ are given by Eq. (33). We assume the relaxation time-scale for $C^{uu}(k;t;t^0)$ and $H_K(k;t;t^0)$ to be $(k)k^2$, while that of $C^{bb}(k;t;t^0)$ and $H_M(k;t;t^0)$ to be $(k)k^2$. The spectrum $C^{(uu;bb)}(k;t;t)$ are written in terms of one-dimensional energy spectra $E^{(u;b)}$ as

$$C^{(uu;bb)}(k;t;t) = \frac{(2)^3}{4k^2} E^{(u;b)} \quad (48)$$

The helicities are written in terms of energy spectra as

$$H_K(k) = r_K k E^u(k) \quad (49)$$

$$H_M(k) = r_M \frac{E^b(k)}{k} \quad (50)$$

Recent numerical simulations [14, 15, 16] and theoretical calculations [9, 10, 11, 13] show that the inertial-range energy spectra $E^{u;b}(k)$ of MHD turbulence follows Kolmogorov's powerlaw (we ignore the intermittency corrections). However in the presence of magnetic helicity, it has been conjectured that the energy spectrum of small wavenumber regime is proportional to k^{-1} due to inverse cascade of magnetic helicity [23]. Therefore, the spectrum of $E^{(u;b)}$ can be taken as

$$E^u(k) = \begin{cases} K^u k^{-2} k^{5=3} & \text{for larger wavenumbers} \\ K^H (H_M)^{2=3} k^{-1} & \text{for smaller wavenumbers} \end{cases} \quad (51)$$

$$E^b(k) = E^u r_A \quad (52)$$

where K^u and H_M are the fluxes of total energy and magnetic helicity respectively. The helicities are taken as in Eqs. (49,50). Also, the renormalized viscosity and resistivity for k^{-1} region will be

$$\left(\nu; \eta\right)(k) = \begin{cases} (K^H)^{1=2} \frac{1=3}{H_M} k^{-1} (\nu; \eta) & \text{for } k < k_n^0 \\ (K^H)^{1=2} \frac{1=3}{H_M} k_n^{-1} (\nu; \eta) & \text{for } k > k_n^0 \end{cases} \quad (53)$$

The parameters ν^0 and η^0 have been calculated using the same procedure as discussed in Subsection III A. The parameters $(\nu; \eta; \nu^0; \eta^0)$ for $r_A = 1$ and $r_A = 5000$ are (1.0, 0.69, 1.07, 0.74) and (0.36, 0.85, 0.46, 0.90) respectively.

We are calculating energy fluxes for the inertial-range wavenumbers where the same powerlaw is valid for all energy spectrum. Therefore, the ratios $r_A; r_M$, and r_K can be treated as constants. A simple dimensional analysis also shows that in the $k^{5=3}$ regime, $(k) = \text{const}$ and $H_M(k)/k^{-1}$, whereas in the k^{-1} regime, $(k)/k$ and $H_M(k) = \text{const}$. We carry out our flux calculation for both the regimes.

We substitute the above forms for the correlation and Green's functions [Eqs. (47-52)], and make the following change of variable:

$$k = \frac{k_0}{u}; p = \frac{k_0}{u}v; q = \frac{k_0}{u}w \quad (54)$$

These operations yield the following nondimensional form of the equation in the $5=3$ region (for details, refer to [3]).

$$\frac{X_{Y>}^{<}(k_0)}{(k_0)} = (K^u)^{3=2} \frac{1}{2} \int_0^1 dv \ln(1=v) \int_{1-v}^{1+v} dw (vw) \sin F_{Y>}^{X<} \quad (55)$$

$$\frac{H_M(k_0)}{(k_0)} = \frac{1}{k_0} (K^u)^{3=2} \frac{1}{2} \int_0^1 dv (1-v) \int_{1-v}^{1+v} dw (vw) \sin F_{H_M} \quad (56)$$

where the integrands $(F_{Y>}^{X<}; F_{H_M})$ are function of $v, w, \nu, \eta, r_A; r_K$ and r_M [3]. In the k^{-1} region, the corresponding equations are

$$1 = \frac{H_M(k_0)}{H_M(k_0)} = (K^H)^{3=2} \frac{1}{2} \int_0^1 dv \ln(1=v) \int_{1-v}^{1+v} dw (vw) \sin F_{H_M} \quad (57)$$

$$\frac{X_{Y>}^{<}(k_0)}{H_M(k_0)} = k_0 (K^H)^{3=2} \frac{1}{2} \int_0^1 dv \frac{1}{v} \int_{1-v}^{1+v} dw (vw) \sin F_{Y>}^{X<} \quad (58)$$

We compute the term in the square brackets, $I_{Y>}^{X<}$, using the similar procedure as that of Verma [3]. We make an assumption however that the interactions are local in wavenumber space. Therefore, most of the contribution to the flux (k_0) comes from the wavenumber shells in the neighbourhood of k_0 . Hence, for computing the flux in $k^{5=3}$ region, we take the energy spectrum for the whole range of integration to be $k^{5=3}$. Similarly assumption is made while calculating the flux for k^1 region.

The flux ratios $\frac{X<}{Y>} =$ can be written in terms of integrals $I_{Y>}^{X<}$, which have been computed numerically. Tables I and II contain their values for $r_A = 1$ and $r_A = 5000$ in both $k^{5=3}$ and k^1 regions. The constants K^u and K^h are calculated using the fact that the total energy flux is sum of all $\frac{X<}{Y>}$. For parameters ($r_A = 5000; r_K = 0.1; r_M = 0.1$), $K^u = 1.55$, while for ($r_A = 1; r_K = 0.1; r_M = 0.1$), $K^u = 0.88$. After this the energy flux ratios $\frac{X<}{Y>} =$ can be calculated. These ratios for some of the specific values of r_A, r_K and r_M are listed in Table III. The first and second terms of $\frac{X<}{Y>} =$ entries are nonhelical and helical components respectively. The flux ratios for parameters ($r_A = 5000; r_K = 0.1; r_M = 0.1$) are also illustrated in Fig. 1.

Using the steady-state condition, we also calculate the energy supply from the large-scale velocity field to the large-scale magnetic field, $\frac{u<}{b<}$. Since magnetic field is not being forced, the energy lost by LS magnetic field through nonhelical channel is compensated by $\frac{u<}{b<}$. That is

$$\frac{u<}{b<} = \frac{b<}{b> \text{ nonhelical}} + \frac{b<}{u> \text{ nonhelical}} \quad (59)$$

An observation of the results shows some interesting patterns. The energy flux can be split into two parts: helical (dependent on r_K and/or r_M) and nonhelical (independent of helicity). The nonhelical part of all the fluxes except $\frac{b<}{u>}$ ($\frac{b<}{u> \text{ nonhelical}} < 0$ for $r_A > 1$) is always positive. As a consequence, in nonhelical channel, ME cascades from LS to SS. Also, since $\frac{u<}{b<} > 0$, LS kinetic energy feeds the LS magnetic energy. The fluxes of nonhelical MHD has been discussed in great detail in paper I.

The sign of $\frac{u<}{u> \text{ helical}}$ is always negative, i.e., kinetic helicity reduces the KE flux. But the sign of helical component of other energy fluxes depends quite crucially on the sign of helicities. From the entries of Table II, we see that

$$\frac{b<}{(b>, u>) \text{ helical}} = ar_M^2 + br_M r_K \quad (60)$$

where a and b are positive constants. If $r_M r_K < 0$, the energy flux to LS magnetic field due to both the terms in the right-hand-side of the above equation is positive. Earlier EDQNM [5] and numerical simulations [18] with forcing of KE and H_K typically have $r_K r_M < 0$. Hence, we can claim that helicity typically induces an inverse energy cascade via $\frac{b<}{b>}$ and $\frac{b<}{u>}$. These fluxes will enhance the large-scale magnetic field.

The flux ratio $H_M =$ can be written in terms of the integrals of Eqs. (56,57) using the same procedure as done for energy flux ratios. The numerical values of the integrals are shown in Tables 1 and 2. Clearly,

$$H_M = dr_M + er_K \quad (61)$$

where d and e are positive constants. Note however that contribution of H_M dominates that of H_K . Clearly the sign of H_M is the same as that of H_K but negative of H_M . From the above equation we observe that positive H_M yields a negative contribution to H_M . Hence, for positive H_M , the magnetic helicity cascade is backward. This result is in agreement with Frisch et al.'s [23] argument in which they predict an inverse cascade of magnetic helicity. Our theoretical result on inverse cascade of H_M is also in agreement with the results derived using EDQNM calculation [5] and numerical simulations [17]. The constant K^h of Eq. (51) can also be calculated using the above procedure. For ($r_A = 5000; r_K = 0.1; r_M = 0.1$), $K^h = 264$, while for ($r_A = 1; r_K = 0.1; r_M = 0.1$), $K^h = 0.78$.

In the following section, we will construct a dynamic dynamo model for galaxies using our flux results.

III. DYNAMO VIA ENERGY AND MAGNETIC HELICITY FLUXES

In the above calculation we have assumed that the turbulence is homogeneous, isotropic, and steady. The assumption of homogeneity and isotropy can be assumed to hold in galaxies in the early phases of evolution before large structures appear. The assumption that the mean magnetic field of galaxy is rather small is valid in the beginning of the galactic evolution. Therefore, we apply the flux obtained from our calculations to estimate the ME growth in galaxies.

During the early phase of galactic evolution, only the LS contain the kinetic and magnetic energies. The fields at these scales interact with each other, but the small-scale spectrum is far from steady (not enough time). The interactions of LS velocity field and the LS seed magnetic field increase the LS seed magnetic field $E^b(t)$ till the steady-state is reached. In absence of helicity, the source of energy for the large-scale magnetic field is $\frac{u<}{b<}$ [Eq. (59)]. When helicity is present, there are several other sources as discussed in section 2 of this paper. Since the forcing of

helicities is effective at LS, it is reasonable to assume that the helical part of $b_{<}^>$ and $u_{<}^>$ will also aid to the increase in LS ME. Hence,

$$\frac{dE^b(t)}{dt} = \frac{u_{<}^>}{b_{<}^>} + \frac{b_{<}^>}{b_{<}^> \text{ helical}} + \frac{u_{<}^>}{b_{<}^> \text{ helical}} \quad (62)$$

We assume a quasi-steady approximation for the early evolution of magnetic field, and substitute the theoretically calculated energy fluxes in the above equation. Since the ME starts with a small value (large r_A limit), all the fluxes appearing in Eq. (62) are proportional to r_A^{-1} [cf. Eqs. (36,38)], i.e.,

$$\frac{u_{<}^>}{b_{<}^>} + \frac{b_{<}^>}{b_{<}^> \text{ helical}} + \frac{u_{<}^>}{b_{<}^> \text{ helical}} = c \frac{E^b}{E^u} \quad (63)$$

where E^u is the LS KE, and c is the constant of proportionality, which depends on the values of helicities. Both Kinetic and magnetic helicities are difficult to ascertain for a galaxy due to lack of observations. We take r_M and r_K to be of the order of 0.1, with r_M being negative. The choice of negative r_M is motivated by the results of EDQNM calculation [5] and numerical simulations [18]. With this value of r_M and r_K , $c = 0.84$ for $E(k)/k^{5=3}$ regime, and $c = 1.3$ for $E(k)/k^{-1}$ regime. Since both the values of constant c is approximately equal and close to 1.0, we take $c = 1.0$ for our calculation. Hence,

$$\frac{1}{L} \frac{dE^b}{dt} = \frac{E^b}{E^u} \quad (64)$$

Using $E^u = K^u L^{2=3} L^{2=3}$, where L is the large length-scale of the system, we obtain

$$\frac{1}{E^u E^b} \frac{dE^b}{dt} = \frac{1}{L (K^u)^{3=2}} \quad (65)$$

We assume that E^u does not change appreciably in the early phase. Therefore,

$$E^b(t) = E^b(0) \exp \left[\frac{1}{L (K^u)^{3=2}} t \right] \quad (66)$$

Hence, the ME grows exponentially in the early periods, and the time-scale of growth is of the order of $L (K^u)^{3=2} = \frac{1}{E^u}$, which is the eddy turnover time [3]. Taking $L = 10^{17}$ km and $\frac{1}{E^u} = 10$ km = sec, we obtain the growth time-scale to be 10^{16} sec or 3×10^8 years, which is in the expected range [22]. Hence, we have constructed a nonlinear and dynamically consistent galactic dynamo based on the energy fluxes. In this model the ME grows exponentially, and the growth time-scale is reasonable [22].

The helical and nonhelical contribution to the fluxes for $r_A = 5000; r_K = 0.1; r_M = 0.1$ is shown in Fig. 1. The flux ratios shown in the figure do not change appreciably as long as $r_A > 100$ or so. As shown in the figure, the three fluxes responsible for the growth of LS ME are $\frac{u_{<}^>}{b_{<}^>} = 2.6 \times 10^{-4}$ (nonhelical), $\frac{b_{<}^>}{b_{<}^> \text{ helical}} = 4.1 \times 10^{-5}$, and $\frac{u_{<}^>}{b_{<}^> \text{ helical}} = 4.0 \times 10^{-5}$. The ratio of nonhelical to helical contribution is $2.6=0.81 \times 3.2$. Hence, the nonhelical contribution is significant, if not more, than the contribution from the helical part for the LS ME amplification. Note that in the earlier papers on dynamo, the helical part is strongly emphasized.

Kulsrad and Anderson (KA) [22] performed an important mean field dynamo calculation of galactic dynamo. Some of the salient features are follows. In KA's kinematic dynamo calculation the growth rate of ME is $\gamma = (1=3) \int k^2 U(k) dk$ where

$$U(k) = \frac{(k)^{2=3} k^{5=3}}{4 k^3 u_k} \quad (k)^{1=3} k^{13=3} \quad (67)$$

KA estimate $k_{\text{max}}^{2=3} (k)^{1=3} = 10^4 \text{ yr}^{-1}$. From this result KA conclude that the kinematic theory predicts a extremely rapid growth of SS ME. The SS noisy magnetic field thus generated will dominate the mean magnetic field that grows at a considerably slower rate (dynamo growth time $\approx 3 \times 10^8 \text{ yr}$). Therefore, it is claimed that the kinematic assumption of the mean dynamo theory is invalid, and it is difficult to build up galactic magnetic field from a very weak seed field using dynamo action.

In contrast, our fully nonlinear and dynamically consistent dynamo is able to generate the observed field from a weak seed magnetic field in a reasonable time scale, which is equal to the eddy turnover time of large eddies of galaxy

($t = L = \frac{P}{E^u}$). To compare with KA's calculation, KA's estimate of growth time-scale is equal to the eddy turnover time of smallest eddies (k_{max}^{-1}). Hence, as pointed out by KA, kinematic assumption is invalid for galactic dynamo, and one has to resort to a dynamical model. Ours is one such theory.

In our model the magnetic energy growth is due to the fluxes $u_{b<}^{u<} + u_{b<helical}^{b>} + u_{b<helical}^{u>}$. In nonhelical MHD, only $u_{b<}^{u<}$ is effective, while in helical MHD both kinetic and magnetic helicities play an important role in the growth of ME. In the current kinematic models of planetary magnetism [1], magnetic field is generated by kinetic helicity, for which planetary rotation (spin) plays an important role. These models appear to work for all the planets except Mercury, which rotates far too slowly. We conjecture that $u_{b<}^{u<}$ (independent of helicities) probably plays an important role in the generation of magnetic field of Mercury.

In helical MHD, the helical contribution to the magnetic energy growth goes as [see Eq. (60)]

$$\frac{dE^b}{dt} = ar_M^2 - br_M r_K \quad (68)$$

where a and b are positive constants. The term ar_M^2 is always positive independent of the sign of H_M , but $br_M r_K$ is positive only when H_M and H_K are of the opposite sign. In numerical simulation of Brandenburg [18] and EDQNM calculation of Pouquet et al. [5], $H_M H_K < 0$ for small k , and $H_M H_K > 0$ for large k . Hence, $br_M r_K$ term is positive for small k , resulting in positive dE^b/dt . Let us compare the above result with the dynamical dynamo of Pouquet et al. [5], Field et al. [7], and Cho [8].

The kinematic dynamo predicts that the growth parameter is proportional to H_K , i.e., $\gamma = u / \eta r_{ui}$. The kinetic model was generalized by Pouquet et al. [5], Field et al. [7], and Cho [8]. In absence of a mean magnetic field they find that

$$\gamma_u + \gamma_b = \gamma_{hu} r_{ui} + \gamma_{hb} r_{bi}; \quad (69)$$

where γ denotes certain time scales (which are always positive). It implies that γ gets positive contribution from both the terms when H_M and H_K are of opposite signs. This result is consistent with Eq. (68). The direct numerical simulation of Pouquet and Patterson [17] indicate that H_M enhances the growth rate of ME considerably, but that is not the case with H_K alone. This numerical result is somewhat inconsistent with results of Pouquet et al. and others [5] (Eq. (69)), but it fits better our formula (68) ($dE^b/dt = 0$ if $r_K = 0$). Hence, our formula (68) probably is a better model for the dynamically consistent dynamo.

In the following section we will summarize our results.

IV. CONCLUSIONS

In this paper we have applied first-order perturbative field theory to calculate the renormalized viscosity, renormalized resistivity, and various cascade rates for helical MHD. We find that the renormalized viscosity and resistivity are unaffected on introduction of both kinetic and magnetic helicities. Our result is consistent with Zhou's calculation [25] for helical uid turbulence.

We find that the energy cascade rates get significantly altered by helicity. Since magnetic helicity is a conserved quantity in MHD, Frisch [23] had argued for k^{-1} energy spectra at small wavenumbers. Keeping this in mind we have calculated energy fluxes for both k^{-1} (small k) and $k^{-5/3}$ (high k) regimes. The fluxes in both the regimes are qualitatively similar. The sign of the fluxes are shown in Fig. 1. The main results of our calculation is as follows:

1. The magnetic energy flux has two components: (a) the nonhelical part which is always positive, (b) the helical part which is negative (assuming $H_M H_K < 0$). The inverse cascade resulting due to helicities is consistent with the results of Pouquet et al. [5], Brandenburg [18], and others.
2. The $u \cdot u$ flux $u_{u>}^{u<}$ gets a inverse component due to kinetic helicity. This implies that KE flux decreases in presence of H_K , a result consistent with that of Kraichnan [28].
3. The growth of large-scale magnetic field in the initial stage of evolution results from $u_{b<}^{u<} + u_{b<helical}^{b>} + u_{b<helical}^{u>}$. In this paper we have computed the relative magnitudes of all three contributions, and find that all of them to be comparable, although $u_{b<}^{u<}$ is somewhat higher. Pouquet et al. [5], Pouquet and Patterson [17], Brandenburg [18], and many others highlight $u_{b<helical}^{b>}$ transfer, and generally do not consider $u_{b<}^{u<}$ and $u_{b<helical}^{u>}$ fluxes.
4. Regarding positive H_M , the flux of magnetic helicity H_M is backward.

Most of the earlier papers (e.g. Pouquet et al. [5]) assume Alfvén time-scale to be the dominant time-scale for MHD turbulence. We have taken nonlinear time-scale (based on Kolmogorov's spectrum) to be the relevant time-scale based on recent numerical [14, 15, 16] and theoretical [9, 10, 11, 12, 13] work.

Using the flux results we have constructed a nonlinear and dynamically consistent galactic dynamo. Our model shows an exponential growth of magnetic energy in the early phase (much before saturation). The growth time-scale is of the order of 3×10^8 years, which is consistent with the current estimate [29]. In our paper we have discussed the growth of magnetic field at scale comparable to forcing scales. In real dynamo, the magnetic field at even larger scales also grow. This growth may be due to inverse cascade of magnetic energy. This problem is beyond the scope of our paper.

Some of the results presented here are general, and they are expected to hold in solar and planetary dynamo. For example, we find that LS velocity field supply energy to LS seed magnetic field. This is one of the sources of dynamo. Hence, if we solve first few MHD modes in spherical coordinate with kinetic forcing, it may be possible to capture some of the salient features of solar and planetary dynamo.

In summary, the energy flux studies of helical MHD provide us with many important insights into the problem of magnetic energy growth. Its application to galactic dynamo yields very interesting results. A generalization of the formalism presented here to spherical geometry may provide us with insights into the magnetic field generation in the Sun and Earth.

Acknowledgments

The author thanks G. Dhar, V. Eswaran, D. Narsimhan, and R. K. Varma for discussions. He also thanks Mustansir Barmia (TIFR, Mumbai) and Krishna Kumar (ISI, Calcutta) for useful suggestions and kind hospitality during his stay in their institutes on his sabbatical leave.

-
- [1] H. K. Moffatt, *Magnetic Fields Generation in Electrically Conducting Fluids* (Cambridge University Press, Cambridge, 1978).
- [2] F. Krause and K. H. Radler, *Mean-Field Magnetohydrodynamics and Dynamo Theory* (Pergamon Press, Oxford, 1980).
- [3] M. K. Verma, *Int. J. Mod. Phys. B* (submitted), nlin.CD/0103033 (2001).
- [4] M. Steenbeck, F. Krause, and K. H. Radler, *Z. Naturforsch.* 21a, 369 (1966).
- [5] A. Pouquet, U. Frisch, and J. Leorat, *J. Fluid Mech.* 77, 321 (1976).
- [6] A. V. Gruzinov and P. H. Diamond, *Phys. Rev. Lett.* 72, 1651 (1994).
- [7] G. B. Field, E. G. Blackman, and H. Chou, *Astrophys. J.* 513, 638 (1999).
- [8] H. Chou, *Astrophys. J.* 552, 803 (2000).
- [9] S. Sridhar and P. Goldreich, *Astrophys. J.* 432, 612 (1994).
- [10] P. Goldreich and S. Sridhar, *Astrophys. J.* 438, 763 (1995).
- [11] M. K. Verma, *Phys. Plasma* 6, 1455 (1999).
- [12] M. K. Verma, *Phys. Rev. E* 64, 26305 (2001).
- [13] M. K. Verma, *Phys. Plasma* 8, 3945 (2001).
- [14] M. K. Verma et al., *J. Geophys. Res.* 101, 21619 (1996).
- [15] W. C. Muller and D. Biskamp, *Phys. Rev. Lett.* 84, 475 (2000).
- [16] D. Biskamp and W. C. Muller, *Phys. Plasma* 7, 4889 (2000).
- [17] A. Pouquet and G. S. Patterson, *J. Fluid Mech.* 85, 305 (1978).
- [18] A. Brandenburg, *Astrophys. J.* 550, 824 (2001).
- [19] P. Frick and D. Sokoloff, *Phys. Rev. E* 57, 4155 (1998).
- [20] G. Dhar, M. K. Verma, and V. Eswaran, *Physica D* 157, 207 (2001).
- [21] M. Meneguzzi, U. Frisch, and A. Pouquet, *Phys. Rev. Lett.* 47, 1060 (1981).
- [22] R. M. Kulsrud and S. W. Anderson, *Astrophys. J.* 396, 606 (1992).
- [23] U. Frisch, A. Pouquet, J. Leorat, and A. Mazure, *J. Fluid Mech.* 68, 769 (1975).
- [24] W. D. McCormack, *The Physics of Fluid Turbulence* (Clarendon, Oxford University Press, 1990).
- [25] Y. Zhou, *Phys. Rev. A* 41, 5683 (1990).
- [26] V. Yakhot and S. A. Orszag, *J. Sci. Comput.* 1, 3 (1986).
- [27] D. C. Leslie, *Development in the Theory of Turbulence* (Clarendon, Oxford University Press, 1973).
- [28] R. H. Kraichnan, *J. Fluid Mech.* 59, 745 (1973).
- [29] A. A. Schekochihin, S. A. Boldyrev, and R. M. Kulsrud, *astro-ph/0103333* (2001).

TABLE I: The values of $I_Y^x = (\frac{x}{Y}) = (K^u)^{1.5}$ calculated using Eqs. (55-58) for A liven ratio $r_A = 1$

	$k^{5=3}$		k^1	
$I_{u>}^{u<}$	0:19	$0:40r_K^2$	0:14	$0:25r_K^2$
$I_{b>}^{u<}$	$0:62 + 0:12r_M^2 + 0:38r_K r_M$		$0:43 + 0:090r_M^2 + 0:20r_K r_M$	
$I_{u>}^{b<}$	0:18	$8:2r_M^2 + 7:7r_K r_M$	0:12	$7:0r_M^2 + 6:8r_K r_M$
$I_{b>}^{b<}$	0:54	$7:6r_M^2 + 8:1r_K r_M$	0:35	$6:6r_M^2 + 7:0r_K r_M$
$I_{b<}^{u<}$	0:73		0:47	
$I_{H_M}^{u<}$	$50r_M + 0:69r_K$		$14r_M + 0:32r_K$	

TABLE II: The values of $I_Y^x = (\frac{x}{Y}) = (K^u)^{1.5}$ calculated using Eqs. (55-58) for A liven ratio $r_A = 5000$

	$k^{5=3}$					k^1				
$I_{u>}^{u<}$	0:53	$1:10r_K^2$				0:32	$0:58r_K^2$			
$I_{b>}^{u<}$	1:9	$10^4 + 5:6$	$10^9 r_M^2 + 8:5$	$10^5 r_K r_M$		1:0	$10^4 + 4:0$	$10^9 r_M^2 + 4:2$	$10^5 r_K r_M$	
$I_{u>}^{b<}$	5:6	10^5	$4:4$	$10^7 r_M^2 + 2:1$	$10^3 r_K r_M$	1:6	10^5	$3:7$	$10^7 r_M^2 + 1:8$	$10^3 r_K r_M$
$I_{b>}^{b<}$	1:4	10^4	$4:1$	$10^7 r_M^2 + 2:1$	$10^3 r_K r_M$	9:8	10^5	$3:5$	$10^7 r_M^2 + 1:8$	$10^3 r_K r_M$
$I_{b<}^{u<}$	$8:8$					$8:2$				
$I_{H_M}^{u<}$	8:2	$10^3 r_M + 1:6$	$10^4 r_K$			2:2	$10^3 r_M + 7:1$	$10^5 r_K$		

TABLE III: The values of energy ux ratios $\frac{x}{Y} =$ for various values of $r_A ; r_K ;$ and r_M for $k^{5=3}$ region. The rst and second entries are nonhelical and helical contributions respectively.

$(r_A ; r_K ; r_M)$	$\frac{u<}{u>} /$	$\frac{u<}{b>} /$	$\frac{b<}{u>} /$	$\frac{b<}{b>} /$	$\frac{u<}{b<} /$
(5000,0.1,-0.1)	(1.0,-0.02)	(3:6 $10^4,$ 1:6 $10^6)$	(1:1 $10^4,$ 4:0 $10^5)$	(2:7 $10^4,$ 4:1 $10^5)$	1:7 10^4
(5000,0.1,0.1)	(1.0,-0.02)	(3:6 $10^4,$ 1:6 $10^6)$	(1:1 $10^4,$ 4:0 $10^5)$	(2:8 $10^4,$ 4:1 $10^5)$	1:7 10^4
(1,0.1,-0.1)	(0.16,-0.0033)	(0.51,-0.0021)	(0.15,-0.13)	(0.44,-0.13)	0.60
(1,0.1,0.1)	(0.12,-0.0026)	(0.4,0.0032)	(0.12,-0.0031)	(0.35,0.0033)	0.47
(1,1,-1)	(0.0062,-0.013)	(0.020,-0.0084)	(0.006,-0.52)	(0.018,-0.51)	0.024
(1,1,1)	(0.11,-0.24)	(0.37,0.30)	(0.11,-0.28)	(0.32,0.30)	0.43
(1,0,1)	(0.014,0)	(0.044,0.0085)	(0.013,-0.58)	(0.038,-0.54)	0.051

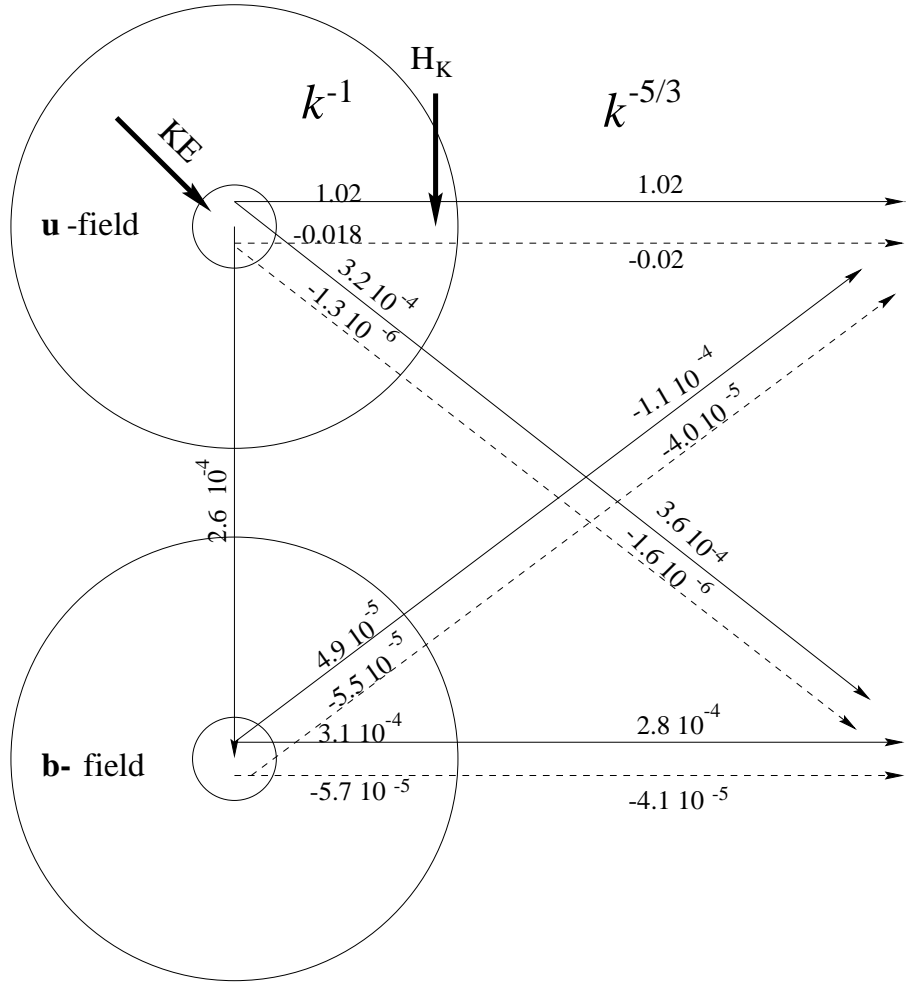


FIG .1: Various energy ux ratios $\frac{x}{y} =$ for helicalMHD for $(r_A = 5000; r_K = 0.1; r_M = 0.1)$. The illustrated wavenumber spheres contain $u <$ and $b <$ modes, while $u >$ and $b >$ are modes outside these spheres. The ux ratios have been calculated for both k^{-1} (small k) and $k^{-5/3}$ (large k) region. The velocity fields is forced at large-scale, and the net input energy is 1 unit. The solid and dashed lines represent the nonhelical and helical contributions respectively.